

Article

Impact of Climate Change on Vegetation Growth in Arid Northwest of China from 1982 to 2011

Rong Zhang¹, Zu-Tao Ouyang², Xiao Xie¹, Hai-Qiang Guo¹, Dun-Yan Tan³, Xiang-Ming Xiao^{1,4}, Jia-Guo Qi² and Bin Zhao^{1,*}

¹ Coastal Ecosystems Research Station of the Yangtze River Estuary, Ministry of Education Key Laboratory for Biodiversity Science and Ecological Engineering, Institute of Biodiversity Science, Fudan University, Shanghai 200438, China; rongzhang1203@gmail.com (R.Z.); xxiieao@gmail.com (X.X.); hqguo@fudan.edu.cn (H.-Q.G.)

² The Center for Global Change & Earth Observations, Michigan State University 218 Manly Miles Building, 1405 S. Harrison Road, East Lansing, MI 48823, USA; zutao.ouyang@gmail.com (Z.-T.O.); qi@msu.edu (J.-G.Q.)

³ Xinjiang Key Laboratory of Grassland Resources and Ecology and Ministry of Education Key Laboratory for Western Arid Region Grassland Resources and Ecology, College of Grassland and Environment Sciences, Xinjiang Agricultural University, Ürümqi 830052, China; tandunyan@163.com

⁴ Department of Microbiology and Plant Biology, Center for Spatial Analysis, University of Oklahoma, Norman, OK 73019, USA; xiangming.xiao@ou.edu

* Correspondence: zhaobin@fudan.edu.cn; Tel.: +86-21-5163-0688; +86-21-5163-0689

Academic Editors: Parth Sarathi Roy and Prasad S. Thenkabil

Received: 3 March 2016; Accepted: 20 April 2016; Published: 27 April 2016

Abstract: Previous studies have concluded that the increase in vegetation in the arid northwest of China is related to precipitation rather than temperature. However, these studies neglected the effects of climate warming on water availability that arise through changes in the melting characteristics of this snowy and glaciated region. Here, we characterized vegetation changes using the newly improved third-generation Global Inventory Modeling and Mapping Studies Normalized Difference Vegetation Index (GIMMS-3g NDVI) from 1982 to 2011. We analyzed the temperature and precipitation trends based on data from 51 meteorological stations across Northwest China and investigated changes in the glaciers using Gravity Recovery and Climate Experiment (GRACE) data. Our results indicated an increasing trend in vegetation greenness in Northwest China, and this increasing trend was mostly associated with increasing winter precipitation and summer temperature. We found that the mean annual temperature increased at a rate of 0.04 °C per year over the past 30 years, which induced rapid glacial melting. The total water storage measured by GRACE decreased by up to 8 mm yr⁻¹ and primarily corresponded to the disappearance of glaciers. Considering the absence of any observed increase in precipitation in the growing season, the vegetation growth may have benefited from the melting of glaciers in high-elevation mountains (*i.e.*, the Tianshan Mountains). Multiple regression analysis showed that temperature was positively correlated with NDVI and that gravity was negatively correlated with NDVI; together, these variables explained 84% of the NDVI variation. Our findings suggest that both winter precipitation and warming-induced glacial melting increased water availability to the arid vegetation in this region, resulting in enhanced greenness.

Keywords: warming; preceding winter precipitation; glacial melting; arid regions

1. Introduction

Ecosystems in arid and semi-arid regions are sensitive to changes in climate [1–5]. Recently, a significant increase in vegetation growth and a change in climate have been observed in Xinjiang, a

typical arid and semi-arid ecosystem located in Northwest China [6–10]. Previous studies indicated that the increased trend of vegetation was related to precipitation rather than temperature [9–11]. However, these studies neglected the potential effects of warming on vegetation growth via the increase in water availability through the melting of snow and glaciers. In arid and semi-arid regions, water availability from precipitation has been reported as the key factor in promoting vegetation growth as a result of reduced water stress [3–5], but a considerable amount of variability in vegetation growth remains unexplained by precipitation alone [9,12–15]. Even if the annual precipitation inputs remain unchanged, the predicted changes in the distribution of precipitation events will impact the timing and quantity of soil water available for plant uptake and biogeochemical processes [16–19]. Local, regional, and global studies all support an increase in winter precipitation in the high latitudes of the Northern Hemisphere [8,20–25], and the higher temperature could increase the rate and intensity of snowmelt. For example, winter precipitation in the form of snow can be an important water resource for vegetation in arid and semi-arid ecosystems as it melts in the spring because it improves moisture conditions and offsets water loss through evapotranspiration [23,26].

Increased precipitation is clearly associated with increased vegetation greenness in arid and semi-arid ecosystems where water is a limited resource [9,12–15]; however, it is unclear why temperature was not found to be an important factor in regulating vegetation in Xinjiang [9]. Higher temperatures can lead to higher productivity provided that other stresses do not intensify [27]. However, warming-induced drought can also decrease vegetation cover/greenness. Therefore, to promote vegetation growth in arid and semi-arid regions, increased precipitation must first offset the increase in drought stress associated with increased temperature in the absence of additional water sources. One important alternative water source is the glacial/snow melt that occurs in snowy areas with large glaciers on high-elevation mountains. Warming temperatures and increasing winter snowfall are expected to increase glacial/snow-derived water in arid and semi-arid regions, which can provide additional water for vegetation [26,28,29]. Knowledge of the responses of glacial melt to climate change is crucial for understanding the water availability for vegetation growth in arid regions. However, to date, only a few studies have investigated the relationship between climate change and glacial melt in the Xinjiang region. The most direct method for studying variations in glaciers and glacial runoff is to monitor changes in the surface mass balance and the equilibrium-line altitude in a small region of a glaciated area [30]. However, due to limited human and financial resources, long-term monitoring is rare, and observations of glacier changes at a regional scale are rarer still.

Temperature has changed more than precipitation in recent decades in Xinjiang [9,11]. It is unclear why this rapid warming trend did not counteract the effects of precipitation in terms of water availability via increased evapotranspiration. Xinjiang is one of the most snowy and glaciated regions in China, and approximately 22,240 glaciers exist in the high-elevation mountains. These glaciers cover an area of 27,974 km² and store approximately 2,814.81 km³ of ice [11,31]. The glaciers are mainly concentrated in the Tianshan and Kunlun Mountains, and glacier melt from these high mountains is a major water source for both humans and natural ecosystems in this region [32]. Recent studies have suggested that glacial melting in the Tianshan Mountains is among the most rapid on Earth due to climate warming [30,31,33]. The resulting water might be an important resource for vegetation under a warming climate for the arid and semi-arid ecosystems near the mountains in Xinjiang. Therefore, we hypothesized that both the increased precipitation and warming-induced glacial melting were associated with the increased vegetation greenness in Xinjiang in recent decades. This hypothesis considers the potential positive effects of changes in both temperature and precipitation on vegetation in this region and motivates us to revisit the possible impacts of climate change on vegetation in the arid northwest of China.

To test our hypothesis, the spatiotemporal changes in vegetation greenness, meteorological conditions, and glacial storage in Xinjiang were comprehensively examined using satellite-observed normalized difference vegetation index (NDVI) data and meteorological data from weather stations from 1982–2011, as well as gravity recovery and climate experiment (GRACE) gravity observations

from 2003–2011. Specifically, we (1) investigated the spatiotemporal changes in the trends of vegetation greenness to determine whether vegetation greenness increased in Xinjiang during this period; (2) investigated the spatiotemporal changes in seasonal precipitation and temperature and their correlations with NDVI to determine the seasons in which climate change was most important; and (3) quantified the empirical relationships between glacier/climate variations and changes in vegetation greenness to test our main hypothesis.

2. Materials and Methods

2.1. Study Area

Xinjiang is located in Northwest China, and it is divided into two large basins by the Tianshan Mountains: the Junggar Basin in the north and the Tarim Basin in the south (Figure 1). The climate in this region is dry because large distances and high mountains (*i.e.*, the Tianshan and Kunlun Mountains, which effectively block atmospheric circulation) separate it from the ocean [11]. The mean annual temperature (MAT) ranges from -4 to 9 °C north of the Tianshan Mountains and from 7 to 14 °C south of the Tianshan Mountains. A significant gradient in annual precipitation (AP) exists from north to south. The AP ranges from 400 to 1000 mm in the Altai Mountains, 100 to 250 mm in the Junggar Basin, 100 to 400 mm in the Tianshan Mountains, and 200 to 300 mm in the Kunlun Mountains. The AP in the Tarim Basin is typically less than 50 mm. The complex geography has led to diverse biomes in the region (Figure 1B).

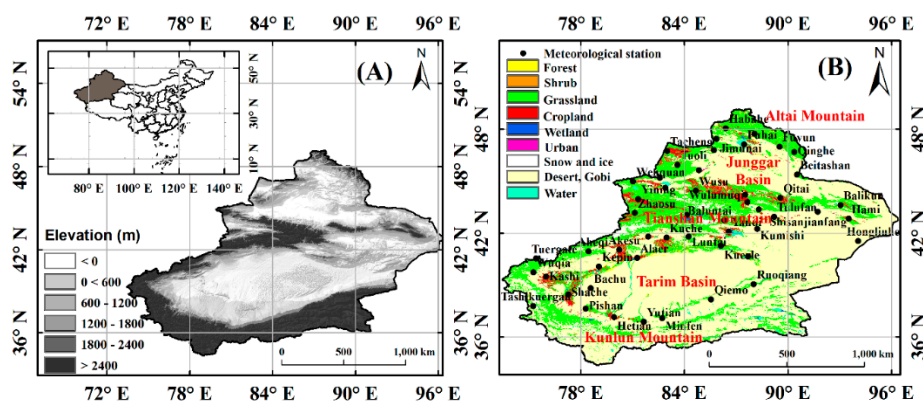


Figure 1. The location of the study area. (A) 1-km Digital Elevation Model of Xinjiang; (B) Spatial distributions of vegetation types and 51 meteorological stations in Xinjiang. The vegetation type dataset is provided by the Environmental & Ecological Science Data Center for West China, National Natural Science Foundation of China (<http://westdc.westgis.ac.cn>).

2.2. AVHRR GIMMS-3g NDVI

We used the NDVI as an indicator of vegetation greenness. This index reflects vegetation growth because it is closely related to the amount of photosynthetically absorbed active radiation [27,34,35]. The newly improved, third-generation Global Inventory Modeling and Mapping Studies (GIMMS-3g) NDVI dataset was obtained from the Advanced Very High Resolution Radiometer (AVHRR) sensors [36–38]. The GIMMS-3g dataset extends the widely used GIMMS dataset, the latter of which is only available for the period of 1981–2006 [35]. The GIMMS-3g dataset covers the period from July 1981 to December 2011 with a spatial resolution of 8 km at 15-day intervals.

We used the larger 15-day NDVI of the two datasets captured each month to produce monthly NDVI datasets that minimize atmospheric effects and cloud contamination effects [27]. To avoid the influence of winter and early spring snow, we only used NDVI data from the growing season (*i.e.*, April to October, NDVI-gs) to compute annual mean NDVI and analyze inter-annual vegetation changes. Grid cells with NDVI values less than 0.05 were masked to exclude sparsely vegetated areas

and extremely dry deserts [34]. Because cropland is influenced by human activity (e.g., irrigation), we masked these areas based on land use/land cover information from 2001 (Figure 1B) when analyzing the response of NDVI-gs to precipitation and temperature changes. However, the vegetation signal from cropland was compared with signals from other vegetated areas to determine the additional effects resulting from human influence. Moreover, cropland and afforestation have both benefited from glacier/snow melt water as well, and irrigation in such areas can reduce GRACE gravity by depleting groundwater. Therefore, when analyzing the relationship between vegetation greenness and the GRACE signal, we considered cropland and afforested areas.

2.3. Climate Data

Climate data were provided by the China Meteorological Data Sharing Service System of the China Meteorological Administration (<http://cdc.nmic.cn/home.do>). Daily mean temperature and precipitation data from 51 available meteorological stations were used to analyze climate trends from 1982 to 2011 (Figure 1B). All 51 meteorological stations had complete daily records from 1982 to 2011. The seasonal/annual precipitation and mean temperature values were calculated to analyze long-term trends. The seasons were defined as Spring, from March to May; Summer, from June to August; Autumn, from September to November; and Winter, from December to February. As there were no meteorological stations in almost a third of the study area (e.g., desert and Gobi regions) and as most stations were distributed in vegetated areas, we did not interpolate the temperature and precipitation data into grids. Snowfall in winter and early spring was included in the precipitation data.

2.4. GRACE

Glacial storage and melting are investigated by using GRACE remote sensing data. GRACE was launched in March 2002 and obtains monthly measurements of changes in the Earth's gravity and therefore changes in mass. In the absence of tectonic movement, mass anomalies are mainly caused by changes in the form of water storage. Therefore, GRACE gravity observations were converted to mass in units of equivalent water thickness to measure the variation in total water storage, which includes groundwater, river discharge, and the water balance of lakes, snow pack, and glaciers [39,40]. We used GRACE to measure glacial storage variations in Xinjiang and particularly the Tianshan Mountains, based on the premise that glacier changes caused by climate warming would overwhelm other water mass changes at a large scale in our study area. Water from melted glaciers was expected to first form surface flow, recharge groundwater and soil water, and then be transferred to other places through runoff and evaporation, causing reduced mass around the glacier region. We noted that irrigation is another important process in Xinjiang that can reduce GRACE gravity by direct pumping of groundwater and subsequent evapotranspiration. The depleted water can be partly recharged by glacier/snow-melted water and thus help accelerate the transfer of water mass originating from glacier/snow outside this region. Meanwhile, heavy irrigation must withdraw previously stored groundwater as well, but it is assumed to be a minor effect compared to glacier retreat because irrigation occurs mainly in cropland and afforested areas, which account for a relatively small area. The GRACE team produces three different solutions (*i.e.*, the Center for Space Research (CSR) at the University of Texas at Austin solution, the German Research Center for Geosciences (GFZ) at Helmholtz Centre Potsdam solution, and the Jet Propulsion Laboratory (JPL) at the California Institute of Technology solution). Due to different data processing methodologies, differences in the three solutions can exist [41]. We therefore used all three versions of the new Release-05 (RL05) Level 2 products. The periods of June 2003 and January and June 2011 are missing in all three products, and December 2011 is missing in the JPL product. GRACE mass anomaly data for all three solutions in the form of equivalent water thickness on a $1 \times 1^\circ$ grid for the land were obtained from the JPL Tellus website [41–43]. Positive GRACE values indicate higher water storage mass than the long-term (2003–2011) average, and negative GRACE values indicate lower water storage mass than the long-term average.

2.5. Statistical Analysis

Ordinary least squares analyses were conducted to estimate linear trends in NDVI-gs, temperature, precipitation, and GRACE mass over the study period, and the statistical significance of these trends was tested via F-tests at the 95% level. To further understand the possible effects of seasonal temperature and/or precipitation on vegetation greenness, these variables were included in multiple regression models to explain the NDVI-gs variation. Winter precipitation in the previous year (PWP) instead of current year winter precipitation was used in these models because vegetation in the growing season can only use water from the previous winter. Akaike's information criterion (AIC) was used to select the optimum linear models among all the possible models. We used AIC instead of R^2 to select our models because AIC is a measure of the relative quality of a statistical model considering both the fitness and the number of parameters. The model with the smallest AIC was selected as the most appropriate model [44]. According to Symonds and Moussalli [45], models with an AIC difference (Δ_i) less than 2 are considered to be essentially equivalent. Thus, all models with Δ_i less than 2 were considered in this study. AIC (Equation (1)) is calculated as

$$AIC = 2k + n \left[\ln \left(\frac{RSS}{n} \right) \right] \quad (1)$$

$$AICc = AIC + 2k(k + 1) / n - k - 1 \quad (2)$$

where k is the number of parameters, RSS is the residual sum of squares of the model, and n is the sample size. When n was less than 40, $AICc$ (Equation (2)), which entails a sample-size correction, was used instead of AIC.

To determine whether glacier melt contributes to the increased greenness of vegetation independent of temperature and precipitation changes, a multiple regression model was constructed in which the GRACE water equivalent thickness along with precipitation and temperature were used to predict NDVI. The monthly anomaly values of these variables during the period from 2003–2011 were used to fit this model. The same criteria based on AIC were used to select the best models among all candidate models. Annual data were not used to fit the model due to the small data size. We also checked whether afforestation and the conversion of natural lands to croplands may have contributed to the decline in GRACE gravity by depleting groundwater (via irrigation) and root-zone water (via evapotranspiration). To check this effect, we plotted the relative percentage of pixels with $NDVI > 0.3$ annually along the GRACE data time series, as a single-year land use map (e.g., Figure 1B) was not sufficient to detect the changes in cropland and afforestation directly. The value 0.3 was selected empirically, as our data shows that the NDVI of other lands rarely exceeds 0.3. To do this, we assumed that an increased number of pixels with annual mean $NDVI > 0.3$ are mainly from cultivated cropland and afforestation.

3. Results

3.1. Linear Trends in Climate and NDVI-gs

Significant changes in NDVI-gs and MAT were observed over the entire study area from 1982 to 2011 (Figure 2a). The NDVI-gs without cropland significantly increased by 0.001 yr^{-1} ($R^2 = 0.77$, $p < 0.001$). The NDVI of cropland was higher and increased at a greater rate (0.0016 yr^{-1} , $R^2 = 0.48$, $p < 0.001$). The MAT increased at a rate of $0.04 \text{ }^\circ\text{C yr}^{-1}$ ($R^2 = 0.41$, $p < 0.001$) during the 30-year period, and especially rapidly after 1997. No significant change was observed in AP ($R^2 = 0.12$, $p = 0.06$). However, a significant increase in precipitation was exclusively observed in winter, with a rate of 0.35 mm yr^{-1} ($p < 0.05$). No obvious trends in the spring ($p = 0.29$), summer ($p = 0.31$), or autumn ($p = 0.27$) precipitation were observed (Figure 2b). All seasonal temperatures except the winter temperature ($p = 0.70$) exhibited significant increasing trends (Figure 2c). The spring and

autumn temperature increased by $0.06\text{ }^{\circ}\text{C yr}^{-1}$ ($p < 0.05$), and the summer temperature increased by $0.04\text{ }^{\circ}\text{C yr}^{-1}$ ($p < 0.05$).

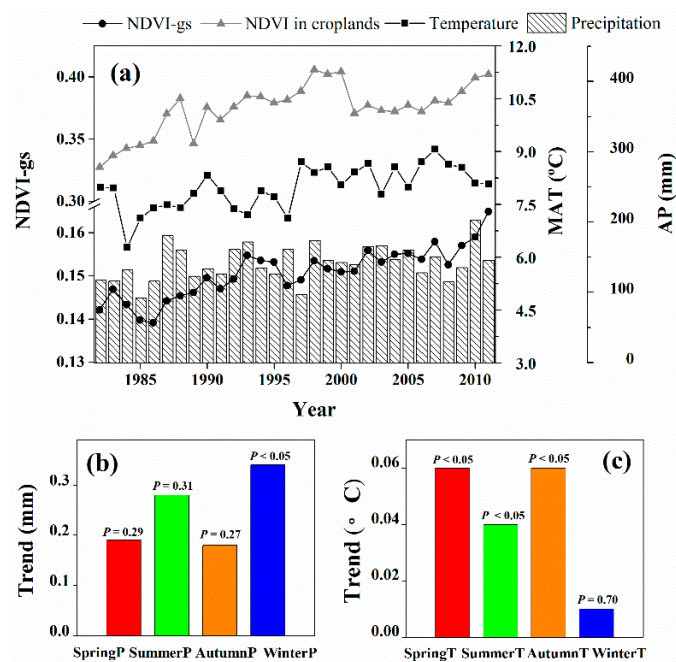


Figure 2. Linear trends in (a) NDVI-gs (Normalized Difference Vegetation Index, where gs refers to the growing season from April to October) without cropland ($y = 0.001x + 0.1417$, $R^2 = 0.77$, $p < 0.001$), NDVI in cropland ($y = 0.0016x + 0.35$, $R^2 = 0.48$, $p < 0.001$), mean annual temperature (MAT, $y = 0.04x - 81.41$, $R^2 = 0.41$, $p < 0.001$), and annual precipitation (AP, $y = 0.99x - 1837.9$, $R^2 = 0.12$, $p = 0.06$) during the period 1982–2011; Trends of (b) seasonal precipitation (mm per year): spring precipitation (spring P, $p = 0.29$), summer precipitation (summer P, $p = 0.31$), autumn precipitation (autumn P, $p = 0.27$), winter precipitation (winter P, $y = 0.34x - 666.7$, $R^2 = 0.29$, $p < 0.05$); and (c) seasonal temperature ($^{\circ}\text{C}$ per year): spring temperature (spring T, $y = 0.06x - 119.1$, $R^2 = 0.25$, $p < 0.05$), summer temperature (summer T, $y = 0.04x - 63.6$, $R^2 = 0.44$, $p < 0.05$), autumn temperature (autumn T, $y = 0.06x - 115.5$, $R^2 = 0.37$, $p < 0.05$), winter temperature (winter T, $p = 0.70$). The analyzed data are from the climate records of 51 meteorological stations.

Three regression models were selected based on our AIC values to explain the inter-annual variations in NDVI-gs at the scale of the whole study area (Table 1). The spring precipitation (spring P), summer temperature (summer T), and preceding winter precipitation (PWP) exhibited close relationships with the changes in NDVI-gs in all of the selected models (Table 1). Among these three variables, PWP possessed the largest standardized regression coefficient (0.49) and explained most of the variation in NDVI-gs compared with spring P (0.10) and summer T (0.17) (Table 1). Summer T presented similar standardized coefficients as spring P but shared more variance with NDVI-gs than did spring P (*i.e.*, a stronger correlation with NDVI-gs) (Table 1). The best regression model with the fewest parameters (Model 1) explained 62% of the inter-annual variation in NDVI-gs. A considerable amount of variability in annual mean NDVI-gs remained unexplained by inter-annual changes in seasonal precipitation and temperature.

Only those models within 2 AIC units were considered comparable. All of the coefficients in this table are reported as standardized coefficients to reflect the relative importance of each predictor within a model. The correlation between each predictor and the NDVI-gs is reported in the bottom row (spring precipitation (spring P), summer temperature (summer T), autumn precipitation (autumn P), winter temperature (winter T), and preceding winter precipitation (PWP)).

Table 1. Regression coefficients of NDVI-gs models with seasonal climate variables from 1982 to 2011 as predictors. AICc refers to Akaike’s information criterion with a sample size correction (see Equation (2)).

Models with Standardized Coefficients					AICc	Δ_i	R ²
1.	NDVI-gs~0.10 spring P + 0.08 summer T + 0.34 PWP				62.7	0.00	0.62
2.	NDVI-gs~0.09 spring P + 0.09 summer T + 0.02 winter T + 0.33 PWP				64.0	1.27	0.63
3.	NDVI-gs~0.07 spring P + 0.08 summer T + 0.02 autumn P + 0.33 PWP				64.1	1.40	0.63
Correlation with NDVI-gs	spring P	summer T	autumn P	winter T	PWP		
	0.32	0.4	0.17	0.01	0.7		

3.2. Spatial Variations in the Climate Variables and NDVI

Most regions of the study area exhibited a significant increasing trend in NDVI-gs ($p < 0.05$) (Figure 3). The highest rate of increase in NDVI-gs occurred in areas surrounding the Tianshan Mountains. Only a few areas exhibited significant negative NDVI-gs trends. These areas were mainly located at the edges of the desert and were associated with an oasis-desert ecotone that is strongly influenced by human activities. A significant increase in AP was observed at only six stations ($p < 0.05$); the remaining 46 stations did not show significant trends in AP from 1982 to 2011 (Figure 4a). Fifteen stations located in the Altai Mountains and at the edge of Junggar Basin showed positive trends in winter precipitation ($p < 0.05$), with rates of 4 mm yr⁻¹ (Figure 4f). Only a few stations in the study area exhibited significant increasing trends in spring P, summer P, and autumn P (Figure 4c–e). In contrast, most stations showed significant increasing trends in spring T, summer T, and autumn T (but not winter T) (Figure 4b,g–i), with rates exceeding approximately 0.04 °C yr⁻¹.

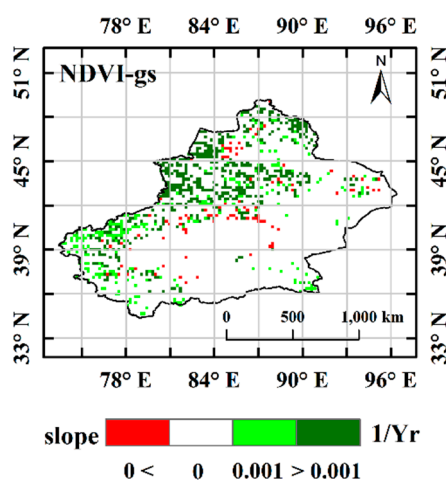


Figure 3. Spatial distribution of growing season NDVI trends from 1982 to 2011 over the Xinjiang region. Areas significant at the 95% level are presented.

3.3. Water Storage Derived from GRACE

The GRACE total water storage estimates revealed that water storage declined in Xinjiang from 2003 to 2011 (Figure 5). All three solutions (*i.e.*, CSR, GFZ, and JPL) showed similar temporal patterns of water storage for the entire study area during the study period (Figure 5). A slight recovery in 2010 was apparent in all three solutions and was consistent with an increase in winter precipitation. Overall, good agreement was observed for the spatial patterns among the three datasets. The largest declines ($p < 0.05$) occurred in the Tianshan Mountain ranges and were as high as 8 mm yr⁻¹, which reflects the disappearance of glaciers at high elevations in the Tianshan Mountains (Figure 6). An increasing trend ($p < 0.05$) was observed in the Kunlun Mountains along the border of Tibet.

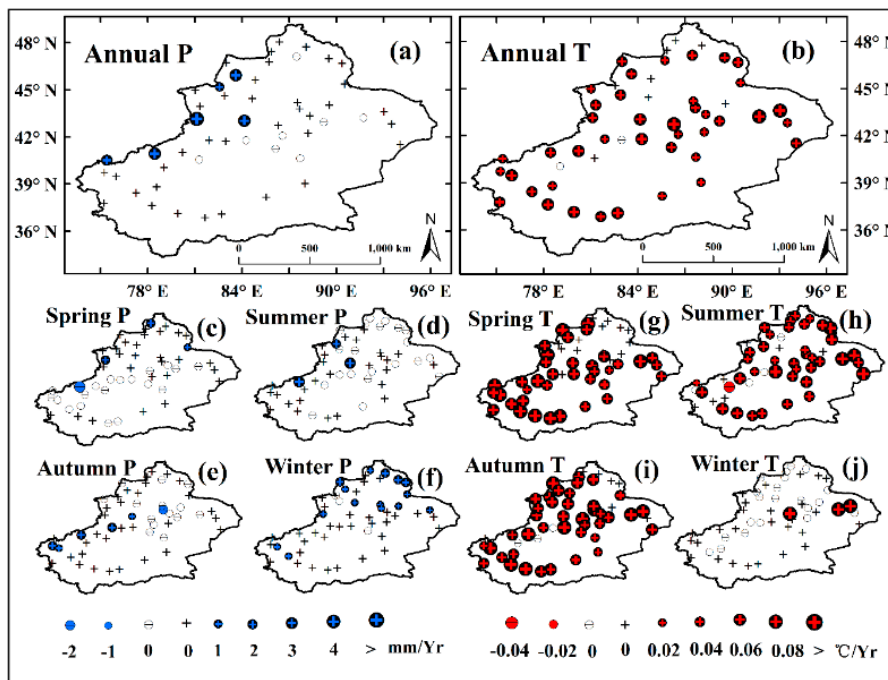


Figure 4. Spatial distribution of trends in precipitation (left) and temperature (right). (a) annual precipitation (annual P); (b) annual temperature (annual T); (c) spring precipitation (spring P); (d) summer precipitation (summer P); (e) autumn precipitation (autumn P); (f) winter precipitation (winter P); (g) spring temperature (spring T); (h) summer temperature (summer T); (i) autumn temperature (autumn T); and (j) winter temperature (winter T) based on 51 meteorological stations from 1982 to 2011. Larger circles indicate stronger increasing/decreasing trends.

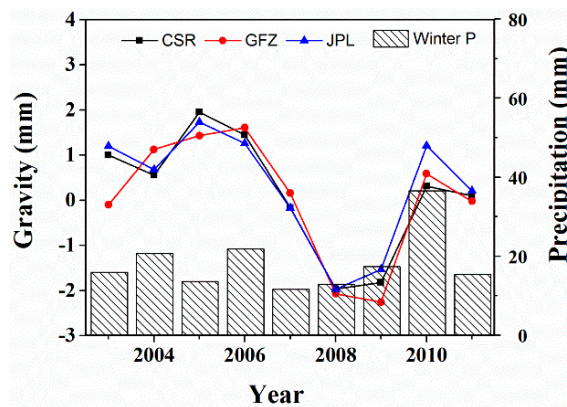


Figure 5. Mean annual GRACE (Gravity Recovery and Climate Experiment) water equivalent thickness in Xinjiang from 2003 to 2011. The histogram represents winter precipitation in mm. GRACE data from all three solutions were plotted: The Center for Space Research (CSR) at the University of Texas at Austin solution, the German Research Center for Geosciences (GFZ) at Helmholtz Centre Potsdam solution, and the Jet Propulsion Laboratory (JPL) at the California Institute of Technology solution.

3.4. Relationships Between Temperature, Precipitation, GRACE, and NDVI

Significant variability in the GRACE water thickness was observed throughout the study area, decreasing yearly during 2003–2011 and corresponding to the increasing trend in NDVI and the increasing trend in the number of pixels with NDVI values greater than 0.3 (Figure 7). Although monthly precipitation, temperature, GRACE total water storage, and the interaction term between GRACE water thickness and temperature were all included in a multiple regression model to predict

NDVI, only temperature and GRACE water thickness (e.g., from the CSR solution) showed significant effects (Table 2). The final best two models, shown in Table 2, explained more than 84% of the variation ($R^2 = 0.84$) in NDVI. In these two models, the removal of temperature decreased the R^2 value to 0.17, and the removal of GRACE water thickness decreased the R^2 value to 0.73, while the removal of precipitation changed less than 0.01 of the R^2 . A significant negative relationship between GRACE water thicknesses and NDVI was observed ($p < 0.05$), whereas a significant positive correlation between temperature and NDVI was observed ($p < 0.05$).

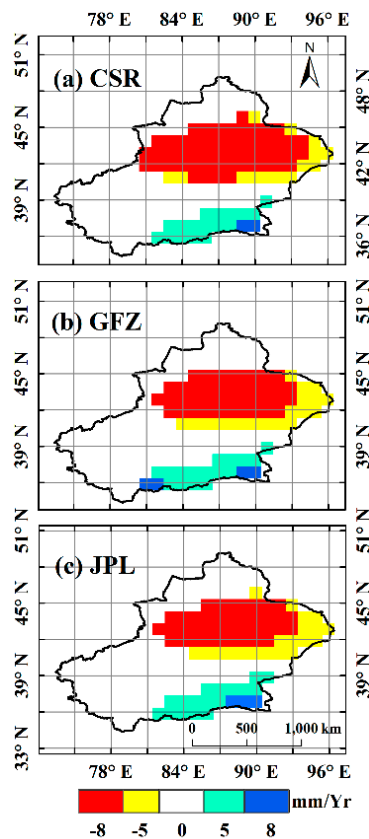


Figure 6. Spatial distribution of GRACE gravity trends in equivalent water thickness based on three solutions: (a) Center for Space Research (CSR); (b) German Research Center for Geosciences (GFZ); and (c) Jet Propulsion Laboratory (JPL). Areas significant at the 95% level are highlighted.

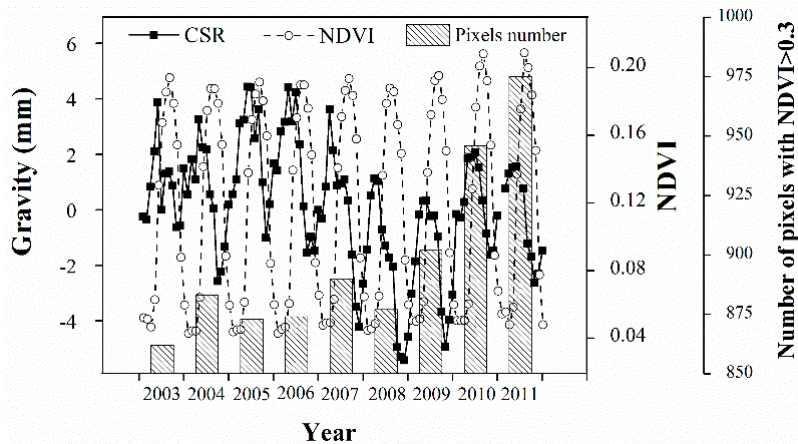


Figure 7. Monthly values in gravity and NDVI from January 2003 to December 2011 in Xinjiang. The histogram represents the pixel number with NDVI values greater than 0.3.

Table 2. Regression coefficients of NDVI models with temperature, precipitation and gravity from 2003 to 2011.

	Models	AICc	Δ_i	R ²
1.	NDVI = 0.0713 + 0.0007P + 0.0037T – 0.0103 CSR	113.1	0.00	0.846
2.	NDVI = 0.0784 + 0.0039T – 0.0104 CSR	113.9	0.81	0.842

4. Discussion

The significant positive NDVI trends observed over most parts of Xinjiang are consistent with previous findings [9,10]. A few locations exhibited significant negative NDVI trends and were mainly located at the edges of deserts (Figure 1) in oasis-desert ecotones greatly influenced by human activities [46,47]. The increasing rate of NDVI observed in this study (0.001 yr^{-1}) is lower than that observed by Zhao and Tan [9] (0.007 yr^{-1}). This difference might be due to the difference in the study period analyzed. The latest AVHRR GIMMS-3g datasets were calibrated with improved algorithms [36–38], and this study excluded agricultural lands that were influenced by irrigation. According to Liu and Kuang [48], cultivation represents one of the major land cover changes in recent decades in Northwest China. Therefore, such areas should be excluded to study the impacts of climate change alone. We minimized the confounding effects of human activity by masking agricultural land. The cropland, however, was increasing at a higher rate due to the combined effects of human interference and changing climate.

Previous studies revealed that increases in annual precipitation were associated with increased vegetation greenness [2,9]; however, we found that the annual precipitation increase was mainly attributable to increased precipitation in the winter. Winter precipitation significantly increased and explained the most NDVI variation compared with the other seasonal climate variables (Figure 2b and Table 1). Winter precipitation played a critical role in regulating vegetation growth, most likely through persistent effects on soil moisture and nutrients [49]. Arid and semi-arid regions are typically water- and nutrient-limited ecosystems, but winter precipitation in the form of snow can provide a large volume of soil water and a large amount of nutrients during the following spring in the form of snowmelt, thereby stimulating seed germination and vegetation growth [20,21]. Winter precipitation in Northwest China consists primarily of snowfall, which can be accumulated and stored. Increased winter snow depth can increase soil microbial activity and nitrogen mineralization rates by increasing soil temperature [50,51], thereby making nutrients available for plant uptake during the winter (e.g., for plants with overwintering roots) and potentially into the growing season [50]. Snowmelt following winter is a slower process compared with rainfall and can thus recharge the soil more effectively and to greater depths [4,52]. Therefore, in Xinjiang, even forested areas, with relatively deeper roots, can benefit from increased winter precipitation. The importance of winter precipitation in vegetation growth is supported by previous studies. For example, shrub abundance in North America was found to increase with an increased proportion of winter precipitation despite a simultaneous decrease in mean annual precipitation [18]. Walker *et al.* [19] found that the aboveground biomass in alpine and arctic ecosystems increased in response to both winter snow and warming. Peng *et al.* [49] found that the mean winter snow depth increased at a rate of $>0.01 \text{ cm yr}^{-1}$ from 1980 to 2005 in this region. Additionally, in Peng *et al.*, snow depth was significantly and positively correlated with NDVI during both the early (May and June) and middle growing seasons (July and August).

Most previous studies have focused on the vegetation impacts of precipitation increases in arid Northwest China [9,11]. However, some of the most severe impacts of climate change are likely to arise from not only the expected increase in precipitation but also the changes in temperature [23,26]. Changes in temperature could lead to important changes in water availability in snowy and glacial areas. Our analysis suggests that increasing summer temperature was important in promoting vegetation greenness (Table 1). Without an increase in precipitation in summer, the increasing temperature in the summer did not decrease vegetation greenness by causing more severe drought

but instead promoted vegetation growth, suggesting that other sources of water might be available. Snow and glacial melting are important hydrologic processes in snow-dominated regions, and changes in temperature are expected to affect the melt characteristics [26,28,29]. We found a rapid decline in total water storage across a large area centered on the high-elevation, glaciated regions of the Tianshan Mountains based on GRACE observations from 2003–2011 (Figure 6). Therefore, we conclude that the glaciers experienced a rapid retreat and that the strong negative signals observed in the surrounding area were likely caused by energy leaking from the glacier center due to the coarse resolution of the GRACE data [28,42]. Other studies have estimated that the glacier area decreased by 1400 km² from 1960 to 1995, with a corresponding increase in glacial melt due to rising temperatures in this region [30]. The annual runoff from glacial melt in the Tianshan Mountains increased 84% from 1958–1985 to 1985–2001 [30]. Therefore, the glacial melting caused by increasing temperature must have provided additional water in addition to direct rainfall, which, when coupled with the increasing temperature, promoted vegetation growth. Cropland and afforested areas use considerable quantities of irrigation water, which involves pumping groundwater and root-zone water into the atmosphere and can contribute to decreases in GRACE gravity values. We have demonstrated that this area has increased since 2003 and that this increase was coupled tightly with the GRACE data (Figure 7). Although irrigated and afforested areas only represent a small portion of the total area, these processes can accelerate the transfer of water originating as glacier/snow to the atmosphere through the discharge process, regardless of the withdrawal of historically stored groundwater. Therefore, although we cannot isolate the effects of groundwater depletion, we have shown its minor effects on reducing total water storage. Furthermore, this does not falsify the previous premise that glacier melting is the main cause of water storage reduction.

To further explore the possible influence of glacial melting on vegetation growth, multiple regression models were conducted to predict NDVI based on the available data from GRACE total water storage observations (Table 2). Although GRACE total water storage was correlated with temperature (*i.e.*, rising temperatures drove glacier melting), the interaction term between the GRACE data and the temperature data did not have a significant effect on NDVI. Temperature was found to be more important than the GRACE data in explaining NDVI variations. This is reasonable because seasonal NDVI variations regulated by temperature were included in the monthly values. However, adding GRACE anomalies to the model significantly increased the R² value by 10%, suggesting that the seasonal changes in the GRACE total water storage were also related to vegetation changes. Because the total water storage change was mainly caused by the accumulation and melting of glaciers and snow (as we assumed and demonstrated), the seasonal melting characteristics of the glaciers could have contributed to the vegetation growth. This conclusion, however, would be more valid if it could be tested over an area without glaciers/snow. A controlled comparison is not possible for such large-scale studies, but findings from other studies can provide supporting evidence. Inner Mongolia experienced no changes in terms of GRACE gravity data in recent decades [28] but did experience climate changes similar to those in Xinjiang [8]. Interestingly, the drylands in Inner Mongolia have exhibited either degradation or no change in vegetation [53,54]. Winter snow occurs in Inner Mongolia, but without glacial/snow accumulation on high-elevation mountains, it cannot be stored until the growing season. If glacial melting were present to provide supplemental water, the vegetation conditions might have experienced improvement rather than degradation.

5. Conclusions

In this study, we presented the spatiotemporal trends of vegetation greenness, annual/seasonal precipitation, and temperature in Northwest China from 1982 to 2011. Linear regression analysis indicated significant positive NDVI-gs and temperature trends over most parts of Xinjiang, consistent with previous studies. We found that total annual precipitation changed little and non-significantly, whereas winter precipitation significantly increased, and the increased vegetation greenness was due to this increase. Due to the lack of observable changes in precipitation during the growing season

throughout the study period, we concluded that climate-warming-induced glacial melting might have provided another source of water for both natural and cultivated vegetation. The results from the GRACE total mass anomaly measurements demonstrated that glaciers experienced rapid melting during 2003–2011 and that the melting was empirically related to the vegetation growth. In general, our results are consistent with our main hypothesis that both increased winter precipitation and warming-induced glacial melting were associated with the increased vegetation greenness in Xinjiang in recent decades. The precipitation increase mainly occurred in the winter, whereas the temperature increase occurred in all seasons except winter. As a result, snow and glacier accumulated mass in the winter and melted during the growing season, thereby promoting vegetation growth.

Acknowledgments: The authors wish to thank Geli Zhang and Lejiang Yu for their constructive comments on the manuscript. This work was supported by the Major National Scientific Research Program of China (2014CB954202) and the National Natural Science Foundation of China (Grant No. U1130301). GRACE land data are available at <http://grace.jpl.nasa.gov>, which is supported by the NASA MEaSUREs Program.

Author Contributions: All authors contributed to the scientific content and authorship of this manuscript.

Conflicts of Interest: The authors declare no conflict of interest.

References

1. Concilio, A.; Chen, J.; Ma, S.; North, M. Precipitation drives interannual variation in summer soil respiration in a Mediterranean-climate, mixed-conifer forest. *Clim. Chang.* **2009**, *92*, 109–122. [[CrossRef](#)]
2. Fang, J.; Piao, S.; Zhou, L.; He, J.; Wei, F.; Myneni, R.B.; Tucker, C.J.; Tan, K. Precipitation patterns alter growth of temperate vegetation. *Geophys. Res. Lett.* **2005**, *32*, L21411. [[CrossRef](#)]
3. Heisler-White, J.L.; Knapp, A.K.; Kelly, E.F. Increasing precipitation event size increases aboveground net primary productivity in a semi-arid grassland. *Oecologia* **2008**, *158*, 129–140. [[CrossRef](#)] [[PubMed](#)]
4. Ogle, K.; Reynolds, J.F. Plant responses to precipitation in desert ecosystems: Integrating functional types, pulses, thresholds, and delays. *Ecosystems* **2004**, *141*, 282–294. [[CrossRef](#)] [[PubMed](#)]
5. Thomey, M.L.; Collins, S.L.; Vargas, R.; Johnson, J.E.; Brown, R.F.; Natvig, D.O.; Friggens, M.T. Effect of precipitation variability on net primary production and soil respiration in a Chihuahuan Desert grassland. *Glob. Chang. Biol.* **2011**, *17*, 1505–1515. [[CrossRef](#)]
6. Folland, C.K.; Karl, T.R.; Christy, J.R.; Clarke, R.A.; Gruba, G.V.; Jouzel, J.; Mann, M.E.; Oerlemans, J.; Salinger, M.J.; Wang, S.W. Observed climate variability and change. In *Climate Change 2001: The Scientific Basis. Contribution of Working Group I to the Third Assessment Report of the Intergovernmental Panel on Climate Change*; Houghton, J.T., Ding, Y., Griggs, D.J., Noguer, M., van der Linden, P.J., Dai, X., Maskell, K., Johnson, C.A., Eds.; Cambridge University Press: New York, NY, USA, 2001; pp. 99–181.
7. Qian, W.; Zhu, Y. Climate change in China from 1880 to 1998 and its impact on the environmental condition. *Clim. Chang.* **2001**, *50*, 419–444. [[CrossRef](#)]
8. Piao, S.; Ciais, P.; Huang, Y.; Shen, Z.; Peng, S.; Li, J.; Zhou, L.; Liu, H.; Ma, Y.; Ding, Y.; *et al.* The impacts of climate change on water resources and agriculture in China. *Nature* **2010**, *467*, 43–51. [[CrossRef](#)] [[PubMed](#)]
9. Zhao, X.; Tan, K.; Zhao, S.; Fang, J. Changing climate affects vegetation growth in the arid region of the northwestern China. *J. Arid Environ.* **2011**, *75*, 946–952. [[CrossRef](#)]
10. Fang, S.; Yan, J.; Che, M.; Zhu, Y.; Liu, Z.; Pei, H.; Zhang, H.; Xu, G.; Lin, X. Climate change and the ecological responses in Xinjiang, China: Model simulations and data analyses. *Quat. Int.* **2013**, *311*, 108–116. [[CrossRef](#)]
11. Shi, Y.; Shen, Y.; Kang, E.; Li, D.; Ding, Y.; Zhang, G.; Hu, R. Recent and future climate change in Northwest China. *Clim. Chang.* **2007**, *80*, 379–393. [[CrossRef](#)]
12. Hsu, J.S.; Powell, J.; Adler, P.B. Sensitivity of mean annual primary production to precipitation. *Glob. Chang. Biol.* **2012**, *18*, 2246–2255. [[CrossRef](#)]
13. Li, Z.; Yan, F.; Fan, X. The variability of NDVI over northwest China and its relation to temperature and precipitation. In Proceedings of 2003 IEEE International Geoscience and Remote Sensing Symposium, IGARSS '03, Beijing, China, 21–25 July 2003.
14. Lázaro, R.; Rodrigo, F.S.; Gutiérrez, L.; Domingo, F.; Puigdefábregas, J. Analysis of a 30-year rainfall record (1967–1997) in semi-arid SE Spain for implications on vegetation. *J. Arid Environ.* **2001**, *48*, 373–395. [[CrossRef](#)]

15. Wang, J.; Rich, P.M.; Price, K.P. Temporal responses of NDVI to precipitation and temperature in the central Great Plains, USA. *Int. J. Remote Sens.* **2003**, *24*, 2345–2364. [[CrossRef](#)]
16. Adler, P.B.; Levine, J.M. Contrasting relationships between precipitation and species richness in space and time. *Oikos* **2007**, *116*, 221–232. [[CrossRef](#)]
17. Guo, Q.; Hu, Z.; Li, S.; Li, X.; Sun, X.; Yu, G. Spatial variations in aboveground net primary productivity along a climate gradient in Eurasian temperate grassland: Effects of mean annual precipitation and its seasonal distribution. *Glob. Chang. Biol.* **2012**, *18*, 3624–3631. [[CrossRef](#)]
18. Paruelo, J.M.; Epstein, H.E.; Lauenroth, W.K.; Burke, I.C. ANPP estimates from NDVI for the central grassland region of the United States. *Ecology* **1997**, *78*, 953–958. [[CrossRef](#)]
19. Walker, M.D.; Walker, D.A.; Welker, J.M.; Arft, A.M.; Bardsley, T.; Brooks, P.D.; Fahnestock, J.T.; Jones, M.H.; Losleben, M.; Parsons, A.N.; *et al.* Long-term experimental manipulation of winter snow regime and summer temperature in arctic and alpine tundra. *Hydrol. Process.* **1999**, *13*, 2315–2330. [[CrossRef](#)]
20. Grippa, M.; Kergoat, L.; Toan, T.L.; Mognard, N.M.; Delbart, N.; Hermitte, J.L.; Vicente-Serrano, S.M. The impact of snow depth and snowmelt on the vegetation variability over central Siberia. *Geophys. Res. Lett.* **2005**, *32*, 2–5. [[CrossRef](#)]
21. Wipf, S.; Stoeckli, V.; Bebi, P. Winter climate change in alpine tundra: Plant responses to changes in snow depth and snowmelt timing. *Clim. Chang.* **2009**, *94*, 105–121. [[CrossRef](#)]
22. Dye, D.G. Variability and trends in the annual snow-cover cycle in Northern Hemisphere land areas, 1972–2000. *Hydrol. Process.* **2002**, *16*, 3065–3077. [[CrossRef](#)]
23. Ragab, R.; Prudhomme, C. Climate change and water resources management in arid and semi-arid regions: Prospective and challenges for the 21st century. *Biosyst. Eng.* **2002**, *81*, 3–34. [[CrossRef](#)]
24. Hamlet, A.F.; Mote, P.W.; Clark, M.P.; Lettenmaier, D.P. Effects of temperature and precipitation variability on snowpack trends in the Western United States. *J. Clim.* **2005**, *18*, 4545–4561. [[CrossRef](#)]
25. Fu, Y.H.; Piao, S.L.; Zhao, H.; Jeong, S.-J.; Wang, X.; Vitasse, Y.; Ciais, P.; Janssens, I.A. Unexpected role of winter precipitation in determining heat requirement for spring vegetation green-up at northern middle and high latitudes. *Glob. Chang. Biol.* **2014**, *20*, 3743–3755. [[CrossRef](#)] [[PubMed](#)]
26. Barnett, T.P.; Adam, J.C.; Lettenmaier, D.P. Potential impacts of a warming climate on water availability in snow-dominated regions. *Nature* **2005**, *438*, 303–309. [[CrossRef](#)] [[PubMed](#)]
27. Wang, X.; Piao, S.; Ciais, P.; Li, J.; Friedlingstein, P.; Koven, C.; Chen, A. Spring temperature change and its implication in the change of vegetation growth in North America from 1982 to 2006. *PNAS* **2011**, *108*, 1240–1245. [[CrossRef](#)] [[PubMed](#)]
28. Jacob, T.; Wahr, J.; Pfeffer, W.T.; Swenson, S. Recent contributions of glaciers and ice caps to sea level rise. *Nature* **2012**, *482*, 514–518. [[CrossRef](#)] [[PubMed](#)]
29. Immerzeel, W.W.; van Beek, L.P.; Bierkens, M.F. Climate change will affect the Asian water towers. *Science* **2010**, *328*, 1382–1385. [[CrossRef](#)] [[PubMed](#)]
30. Liu, S.; Sun, W.; Shen, Y.; Li, G. Glacier changes since the Little Ice Age maximum in the western Qilian Shan, northwest China, and consequences of glacier runoff for water supply. *J. Glaciol.* **2003**, *49*, 117–124.
31. Liu, S.; Ding, Y.; Shangguan, D.; Zhang, Y.; Li, J.; Han, H.; Wang, J.; Xie, C. Glacier retreat as a result of climate warming and increased precipitation in the Tarim river basin, northwest China. *Ann. Glaciol.* **2006**, *43*, 91–96. [[CrossRef](#)]
32. Wang, X.; Xie, H.; Liang, T. Evaluation of MODIS snow cover and cloud mask and its application in Northern Xinjiang, China. *Remote Sens. Environ.* **2007**, *112*, 1497–1513. [[CrossRef](#)]
33. Yao, T. Recent glacial retreat in High Asia in China and its impact on water resource in Northwest China. *Sci. China Ser. D* **2004**, *47*, 1065–1075. [[CrossRef](#)]
34. Slayback, D.A.; Pinzon, J.; Los, S.O.; Tucker, C.J. Northern hemisphere photosynthetic trends 1982 ± 99. *Glob. Chang. Biol.* **2003**, *9*, 1–15. [[CrossRef](#)]
35. Tucker, C.J.; Pinzon, J.E.; Brown, M.E.; Slayback, A.; Pak, E.W.; Mahoney, R.; Vermote, E.F.; Saleous, N.E.L. An extended AVHRR 8-km NDVI dataset compatible with MODIS and SPOT vegetation NDVI data. *Int. J. Remote Sens.* **2005**, *26*, 4485–4498. [[CrossRef](#)]
36. Guay, K.C.; Beck, P.S.A.; Berner, L.T.; Goetz, S.J.; Baccini, A.; Buermann, W. Vegetation productivity patterns at high northern latitudes: A multi-sensor satellite data assessment. *Glob. Chang. Biol.* **2014**, *20*, 3147–3158. [[CrossRef](#)] [[PubMed](#)]

37. Zhu, Z.; Bi, J.; Pan, Y.; Ganguly, S.; Anav, A.; Xu, L.; Samanta, A.; Piao, S.; Nemani, R.; Myneni, R. Global Data Sets of Vegetation Leaf Area Index (LAI)_{3g} and Fraction of Photosynthetically Active Radiation (FPAR)_{3g} Derived from Global Inventory Modeling and Mapping Studies (GIMMS) Normalized Difference Vegetation Index (NDVI)_{3g} for the Period 1981 to 2011. *Remote Sens.* **2013**, *5*, 927–948.
38. Dardel, C.; Kergoat, L.; Hiernaux, P.; Grippa, M.; Mougin, E.; Ciais, P.; Nguyen, C.-C. Rain-Use-Efficiency: What it Tells us about the Conflicting Sahel Greening and Sahelian Paradox. *Remote Sens.* **2014**, *6*, 3446–3474. [[CrossRef](#)]
39. Swenson, S.; Famiglietti, J.; Basara, J.; Wahr, J. Estimating profile soil moisture and groundwater variations using GRACE and Oklahoma Mesonet soil moisture data. *Water Resour. Res.* **2008**, *44*, W01413. [[CrossRef](#)]
40. Swenson, S.; Wahr, J. Monitoring the water balance of Lake Victoria, East Africa, from space. *J. Hydrol.* **2009**, *370*, 163–176. [[CrossRef](#)]
41. Landerer, F.W.; Swenson, S.C. Accuracy of scaled GRACE terrestrial water storage estimates. *Water Resour. Res.* **2012**, *48*. [[CrossRef](#)]
42. Swenson, S.; Wahr, J. Post-processing removal of correlated errors in GRACE data. *Geophys. Res. Lett.* **2006**, *33*. [[CrossRef](#)]
43. GRACE Tellus. Available online: <http://grace.jpl.nasa.gov/data/get-data/monthly-mass-grids-land/> (accessed on 01/12/2015).
44. Yamaoka, K.; Nakagawa, T.; Uno, T. Application of Akaike's Information Criterion (AIC) in the evaluation of linear pharmacokinetic equations. *J. Pharmacokinet. Biopharm* **1978**, *6*, 165–175. [[CrossRef](#)] [[PubMed](#)]
45. Symonds, M.R.E.; Moussalli, A. A brief guide to model selection, multimodel inference and model averaging in behavioural ecology using Akaike's information criterion. *Behav. Ecol. Sociobiol.* **2011**, *65*, 13–21. [[CrossRef](#)]
46. Su, Y.Z.; Zhao, W.Z.; Su, P.X.; Zhang, Z.H.; Wang, T.; Ram, R. Ecological effects of desertification control and desertified land reclamation in an oasis-desert ecotone in an arid region: A case study in Hexi Corridor, northwest China. *Ecol. Eng.* **2007**, *29*, 117–124. [[CrossRef](#)]
47. Zu, R.; Gao, Q.; Qu, J.; Qiang, M. Environmental changes of oases at southern margin of Tarim Basin, China. *Environ. Geol.* **2003**, *44*, 639–644. [[CrossRef](#)]
48. Liu, J.; Kuang, W.; Zhang, Z.; Xu, X.; Qin, Y.; Ning, J.; Zhou, W.; Zhang, S.; Li, R.; Yan, C.; *et al.* Spatiotemporal characteristics, patterns, and causes of land-use changes in China since the late 1980s. *J. Geogr. Sci.* **2014**, *24*, 195–210. [[CrossRef](#)]
49. Peng, S.; Piao, S.; Ciais, P.; Fang, J.; Wang, X. Change in winter snow depth and its impacts on vegetation in China. *Glob. Chang. Biol.* **2010**, *16*, 3004–3013. [[CrossRef](#)]
50. Liston, G.E.; Sturm, M. Winter precipitation patterns in Arctic Alaska Determined from a blowing-snow model and snow-depth observations. *J. Hydrometeorol.* **2002**, *3*, 646–659. [[CrossRef](#)]
51. Schimel, J.P.; Bilbrough, C.; Welker, J.M. Increased snow depth affects microbial activity and nitrogen mineralization in two Arctic tundra. *Soil Biol. Biochem.* **2003**, *36*, 217–227. [[CrossRef](#)]
52. Walter, H. Natural savannahs as a transition to the arid zone. In *Ecology of Tropical and Subtropical Vegetation*; Heinrich, W., Mueller-Dombois, D., Eds.; Oliver & Boyd: Edinburgh, UK, 1971; pp. 238–265.
53. Ma, W.; Liu, Z.; Wang, Z.; Wang, W.; Liang, C.; Tang, Y.; He, J.; Fang, J. Climate change alters interannual variation of grassland aboveground productivity: Evidence from a 22-year measurement series in the Inner Mongolian grassland. *J. Plant Res.* **2010**, *123*, 509–517. [[CrossRef](#)] [[PubMed](#)]
54. Peng, S.; Chen, A.; Xu, L.; Cao, C.; Fang, J.; Myneni, R.B.; Pinzon, J.E.; Tucker, C.J.; Piao, S. Recent change of vegetation growth trend in China. *Environ. Res. Lett.* **2011**, *6*, 044027. [[CrossRef](#)]

